EurJIC
European Journal of Inorganic Chemistry

Full Paper
doi.org/10.1002/ejic.202000195

Chemistry Europe
European Chemical Societies Publishing

Lanthanide Polychalcogenides

Transport Properties of $GdTe_{1.8-x}As_x$ (x = 0, 0.04)

Hagen Poddig,[a,b] Dean Hobbis,[b] Noha Alzahrani,[b] Thomas Doert,[a] and George S. Nolas*[b]

Abstract: Phase-pure polycrystalline samples of $GdTe_{1.8}$ and $GdTe_{1.76}As_{0.04}$ were synthesized by reacting Gd_2Te_3 with elemental Te and As, employing a small amount of I_2 as mineralizer. Polycrystalline specimens were densified by SPS for temperature dependent electrical and thermal properties investigations. The electrical properties indicate that arsenic doping leads to a change from n- to p-type conduction, with an order-of-magnitude reduction in resistivity with As doping at room-temperature as compared to $GdTe_{1.8}$. The thermal conductivity of both specimens is low, the result of the crystal structure and atypical Te bonding in this material. The results presented are intended to expand on the research into rare-earth polychalcogenides and advance the fundamental investigation of these materials, as well as begin to evaluate their potential for thermoelectric applications.

Introduction

Several studies report on the structural chemistry of rare-earth metal polychalcogenides $REX_{2-\delta}$ (X = S, Se, Te) ($0 \le \delta \le 0.2$) featuring trivalent RE metals (RE = Y, La–Nd, Sm, Gd–Lu). The first structure proposed for $LaTe_2$ involved the space group $P4/nmm$ (No. 129) with a = 450.7(5) pm and c = 913(1) pm in 1966.[1] Further studies, however, revealed a more complex (super)structure, as described by Stöwe, with space group Pc (No. 7) and lattice parameters a = 919.0(1) pm, b = 910.7(1) pm, c = 907.0(1) pm and β = 90.04(1)°, indicating a monoclinic distortion in this compound.[2] The aristotype for most of the rare earth metal polychalcogenides $REX_{2-\delta}$[3] is the structure of ZrSSi,[4,5] which shows an alternating stacking of a puckered [ZrS] layer and a square planar layer of [Si]. Analogous to the structure of ZrSSi, $REX_{2-\delta}$ compounds show the same alternating stacking of puckered [REX] layers and planar [X] layers, the latter having a clear distortion from a square net that can be explained by the formation of X_2^{2-} anions if RE is a trivalent metal. This results in shorter interatomic distances in the X_2^{2-} anions and larger distances between them. The sulfides and selenides have been intensively investigated, for example high-temperature high-pressure experiments have been employed to reach pressure stabilized phases of the smaller rare earth metals in REX_2 (RE = Sm, Gd–Tm, X = S, Se)[6] and $REX_{1.9}$ (RE = Gd–Tm, X = S, Se).[7] The corresponding tellurides have been investigated less and the reported structures of the stoichiometric $RETe_2$ (RE = La, Ce, Pr) compounds differ from those of the analogous rare-earth metal sulfides and selenides,[2,8,9] although $CeTe_{1.9}$ crystallizes in the $CeSe_{1.9}$ structure type that is common to the corresponding sulfides and selenides.[10]

An atypical structure type in this class of compounds is observed for the tellurides with composition $RETe_{1.8}$ (RE = Sm, Gd–Dy).[10–13] The crystal structure of $GdTe_{1.8}$ can be described by a $\sqrt{5}\times\sqrt{5}\times2$ superstructure of the basic tetragonal unit cell, as in the ZrSSi aristotype, but crystallizing in space group $P4/n$ (No. 85) with a = 966.10(4) pm and c = 1794.2(1) pm.[13] The doubling of the c-axis results in two stacks of puckered [GdTe] layers and a planar [Te] layer per unit cell, with a unique [Te] layer as compared to the known sulfides and selenides. This [Te] layer comprises two statistically disordered Te_2^{2-} dumbbells that are surrounded by four linear Te_3^{4-} units. This linear Te_3 unit reacts to the statistical ordering of the Te_2^{2-} dumbbell with a small displacement of the outer Te atoms of the linear entity, as indicated by a large anisotropic displacement parameter.[13] This type of structural "disorder" would presumably cause strong phonon scattering resulting in a relatively low thermal conductivity, and is one reason for our interest in these materials.

The physical properties of the $RETe_{2-\delta}$ compounds have been primarily investigated for $LaTe_2$ and $CeTe_2$, including magnetization,[8,14,15] electronic structure,[16,17] optical[18–20] and transport properties.[21,22] The cubic Th_3P_4-phases $La_{3-x}Te_4$, Ce_3Te_4, $Pr_{3-x}Te_4$ and $Nd_{3-x}Te_4$ have also been investigate for potential thermoelectric applications, particularly at high temperatures.[23–26] Due to the complex structural chemistry of $RETe_{2-\delta}$ and the oxophilic behavior of the rare earth metals, the number of reports on the physical properties and applications of these materials are limited. Recently, the synthesis and the crystal structures of $RETe_{1.8}$ with RE = Gd, Tb, Dy have been described, including the electronic properties of $GdTe_{1.8}$.[13] In the present report, we have synthesized $GdTe_{1.8}$ and investigated its temperature dependent electrical and thermal transport properties.

[a] H. Poddig, Prof. Dr. T. Doert
Faculty of Chemistry and Food Chemistry, Technische Universität Dresden, 01062 Dresden, Germany
[b] H. Poddig, D. Hobbis, N. Alzahrani, Prof. Dr. G. S. Nolas
Department of Physics, University of South Florida, Tampa, FL, 33620, USA
E-mail: gnolas@usf.edu
http://shell.cas.usf.edu/gnolas/
ORCID(s) from the author(s) for this article is/are available on the WWW under https://doi.org/10.1002/ejic.202000195.

Full Paper
doi.org/10.1002/ejic.202000195

In addition, an As-doped specimen was synthesized and measured in order to compare with that of $GdTe_{1.8}$. This work aims for a better understanding of the largely unstudied transport properties of tellurium deficient compounds $RETe_{2-\delta}$, as well as the impact of doping on these properties.

Results and Discussion

The structure of $GdTe_{1.8}$ is described in detail elsewhere,[13] however neither doping nor stoichiometric substitution have been reported previously, to the best of our knowledge. There are, however, reports on mixed transition metal pnictides chalcogenides.[27–31] From a chemical perspective, the elements with lowest and highest electronegativity should preferably constitute the puckered [*REX*] layers whereas the planar [*X*] layer comprise the medium electronegative elements.[32] Such site preferences were indeed observed in the mixed sulfides and selenides $LaS_{2-x}Se_x$,[33] $LaS_{1.9-x}Se_x$[34] and in the mixed tellurium antimony compound $GdSb_xTe_{2-x-\delta}$ compound where the planar [*X*] layer is mainly composed of (the medium electronegative) Sb.[35–37,38] Regardless of the reference, As (2.18,[35] 2.211,[36] 2.20[37]) is more electronegative than Te (2.1,[35] 2.158,[36] 2.01[37]), suggesting a substitution on the anion site in the [GdTe] layer without changing the structure of the [Te] layers (Figure 1). However, GdAsTe, which could be considered as the limiting As-rich end-member of a hypothetical substitution series $GdTe_{2-x}As_x$, adopts the TiNiSi structure (space group *Pnma*) that is comprised of zigzag chains of As.[39] Our XRD data on $GdTe_{1.76}As_{0.04}$, however, do not align with the TiNiSi structure type.

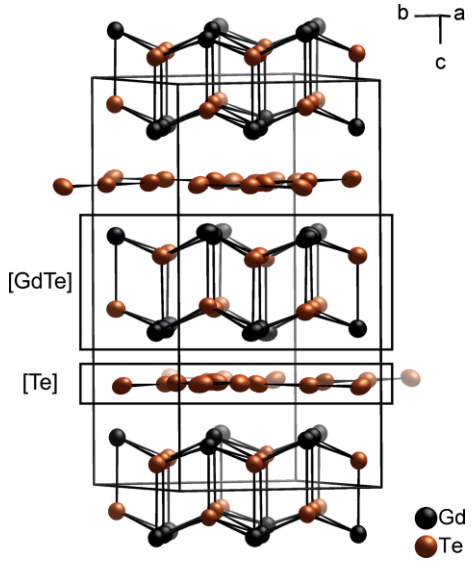

Figure 1. Crystal structure of $GdTe_{1.8}$ with the [GdTe] and [Te] layer marked. Substitution of As is expected in the [GdTe] layer.

The synthesis route of $GdTe_{1.8-x}As_x$ was adjusted from that previously report for $GdTe_{1.8}$[13] by starting from the gadolinium sesquitelluride Gd_2Te_3 and adding a stoichiometric amount of tellurium and arsenic to the reaction mixture, as show in equation (1).

$$Gd_2Te_3 + 0.6 - x\,Te + x\,As \xrightarrow{I_2} 2\,GdTe_{1.8-x}As_x \qquad (1)$$

The powder XRD pattern for $GdTe_{1.8}$ and the As-doped specimen show no evidence of impurities or distortions from the ideal $GdTe_{1.8}$ structure (Figure 2). Le Bail profile fitting of the powder pattern suggests only a very small reduction in the *c* parameter of the As-doped compound with respect to the binary telluride, which can be attributed to the smaller size of the As atoms (considering atomic radii, e.g.: r_{As} = 115 pm, r_{Te} = 140 pm).[40]

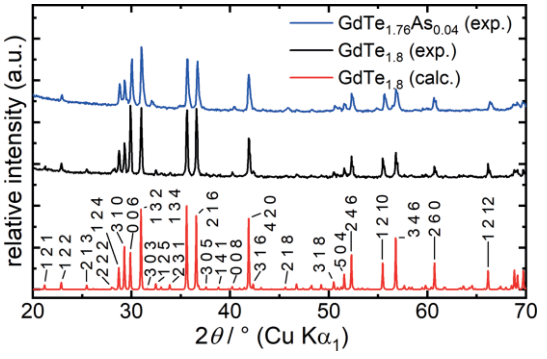

Figure 2. PXRD patterns of $GdTe_{1.8}$ and $GdTe_{1.76}As_{0.04}$ with comparison to the calculated diffraction pattern of $GdTe_{1.8}$ (CSD-1864760) with space group *P4/n*.

The temperature dependent electrical resistivity, ρ, (Figure 3a) of $GdTe_{1.8}$ and $GdTe_{1.76}As_{0.04}$ show characteristic semiconductor behavior, in agreement with previous results on $GdTe_{1.8}$.[13] The band-gap, E_g, can be estimated from the highest temperature ρ values using a fit of the form $\rho = \rho_0\ exp(E_g/2k_BT)$ where k_B is the Boltzmann constant and *T* is the absolute temperature. This results in an estimated E_g of 0.24 eV for $GdTe_{1.8}$, in agreement with E_g = 0.19 eV reported previously.[13]

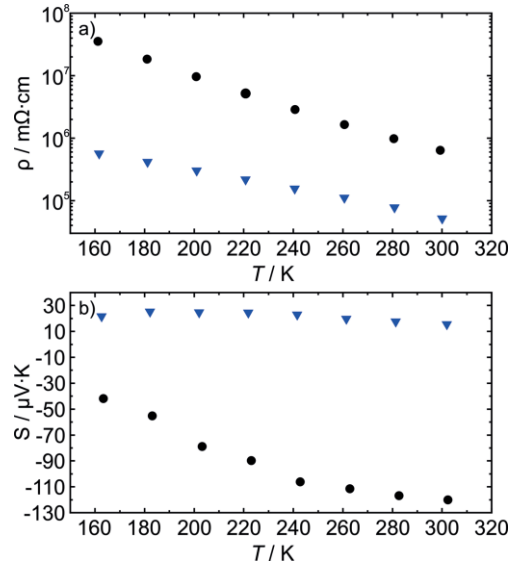

Figure 3. Temperature dependent (a) ρ and (b) *S* for $GdTe_{1.8}$ (circle) and $GdTe_{1.76}As_{0.04}$ (triangle).

Full Paper
doi.org/10.1002/ejic.202000195

The As-doped specimen has lower ρ values as compared to $GdTe_{1.8}$, with an order of magnitude decrease at room temperature as shown in Figure 2, due to As doping. The estimated E_g for $GdTe_{1.76}As_{0.04}$ is 0.23 eV, a value that is similar to that of $GdTe_{1.8}$. Furthermore, a change from n-type to p-type conduction upon As doping was observed; the S values for $GdTe_{1.8}$ are negative, indicating n-type conduction, while the S values for $GdTe_{1.76}As_{0.04}$ are positive, indicating p-type conduction. The S values for the As-doped specimen are small with a relatively flat temperature dependence over the measured temperature range.

The κ values for both specimens (Figure 4) are relatively low and comparable to Bi_2Te_3 alloys and other chalcogenides, e.g. $Nd_{3-x}Te_4$, that have been investigated for potential thermoelectric applications.[26,41–44] However, they indicate different temperature dependencies. The temperature dependence of κ for $GdTe_{1.8}$ shows a decrease in κ with decreasing temperature. This atypical temperature dependence would result from the disordered Te_2^{2-} dumbbell arrangement of Te in the crystal structure that presumably provides strong phonon scattering. Furthermore, $GdTe_{1.76}As_{0.04}$ seems to possess a more typical dielectric temperature dependence, possibly due to As doping which shortens the distances inside the $[GdTe_{1-x}As_x]$ layer, as discussed above. The shorter Gd–As distances would influence the vibrations in the [GdTe] layer by affecting the bonding situation, which should have a more ionic character than the Gd–Te bond, due to the higher electronegativity even for low concentrations. In terms of the magnitude of κ, however, As doping does not significantly change the κ values in $GdTe_{1.8}$. The low κ values are intrinsic to this material system and can be attributed to the complex crystal structure and it's anion disorder.

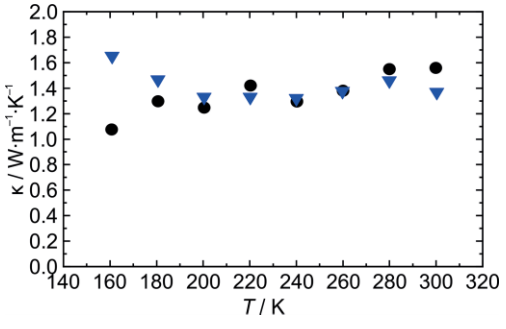

Figure 4. Temperature dependent κ for $GdTe_{1.8}$ (circle) and $GdTe_{1.76}As_{0.04}$ (triangle).

Conclusion

The temperature dependent electrical and thermal properties of $GdTe_{1.8}$ are reported. Our results indicate the transport properties of $GdTe_{1.8}$ are sensitive to doping, as illustrated by the change from n-type to p-type conduction as well as a change in the temperature dependence of κ with a small concentration of As doping. This material has intrinsically low κ values attributable to the complex crystal structure. Although the thermoelectric figure of merit ZT ($= S^2T/\rho\kappa$) for these compositions is small, the sensitivity to doping as well as the low κ values indicates that these materials should be of interest for further investigation as potential thermoelectric materials.

Experimental Section

All preparatory steps for the synthesis were carried out in a nitrogen filled glovebox. A small amount of iodine (≈ 0.02 equivalents to $GdTe_{1.8}$) was added to the reaction mixture to enhance the mass transport and to ensure a complete reaction. In a standard synthesis, 3 g of a stoichiometric mixture of Gd_2Te_3 and tellurium (Alfa Aesar, 99.999 %), and As (Alfa Aesar, 99.9 %) for the As-doped composition, were placed in a quartz tube and sealed under dynamic vacuum ($p \leq 1 \times 10^{-3}$ mbar). The reaction mixture was heated to 1073 K and held at this temperature for 5 days. The prepared specimens were stored and handled in a nitrogen atmosphere. The precursor Gd_2Te_3 was prepared analogously by reacting elemental Gd (99.5 %, MaTecK) and Te (Merck, > 99.9 %, reduced in H_2 stream at 400 °C) in a glassy carbon crucible inside a fused silica ampoule. The fine ground powder was heated to 1073 K and held at this temperature for 4 days. The ampoule was opened in an argon filled glovebox and the purity of the precursor was checked by X-ray powder diffraction.

Powder X-ray diffraction (PXRD) data of the synthesized, powdered specimens were collected on a Bruker D8 focus diffractometer in Bragg–Brentano geometry with Cu-K_α radiation and a graphite receiving monochromator. The specimens were ground into fine powder, sieved (325 mesh) and placed inside a custom-designed WC die and punch assembly that was lined with graphite foil to prevent reactions with the surrounding material for densification. Densification was performed by spark plasma sintering (SPS) under vacuum at 523 K and 400 MPa for 30 minutes. The maximum temperature for densification was evaluated by differential thermal analysis (DTA) and thermal gravimetric analysis (TGA) using a TA Instruments Q600 to ensure that the specimens did not undergo oxidation or degradation during the densification process.

Temperature dependent transport measurements were performed on $2 \times 2 \times 5$ mm^3 parallelepipeds that were cut using an abrasive slurry wire saw. Low-temperature four-probe gradient measurements (160–300 K) on resistivity, ρ, Seebeck coefficient, S, and steady state thermal conductivity, κ, were performed on a custom built radiation-shielded vacuum probe.[45,46] The electrical contacts were made by directly soldering to Ni plated surfaces and Stycast epoxy was used for the thermal contacts. The maximum experimental uncertainties for these measurements are 7 % for ρ, 6 % for S and 8 % for κ measurements.

CCDC 1864760 contain(s) the supplementary crystallographic data for this paper. These data are provided free of charge by the joint Cambridge Crystallographic Data Centre and Fachinformationszentrum Karlsruhe Access Structures service www.ccdc.cam.ac.uk/structures.

Acknowledgments

This work was supported by the ERASMUS+ ICM WORLDWIDE exchange program funded by the European Union. Financial Support by the German Research Foundation (DFG, grants no. Do 590/6-1) is gratefully acknowledged. GSN acknowledges the support of the US National Science Foundation under grant No. DMR-1748188. DH acknowledges the II-VI Foundation Block-Gift Program.

Keywords: Lanthanide metal polytellurides · Transport properties · Semiconductors

[1] R. Wang, H. Steinfink, W. F. Bradley, *Inorg. Chem.* **1966**, *5*, 142–145.
[2] K. Stöwe, *J. Solid State Chem.* **2000**, *149*, 155–166.
[3] T. Doert, C. J. Müller, in *Reference Module in Chemistry, Molecular Sciences and Chemical Engineering*, Elsevier, **2016**.
[4] H. Onken, K. Vierheilig, H. Hahn, *Z. Anorg. Allg. Chem.* **1964**, *333*, 267–279.
[5] A. Klein Haneveld, F. Jellinek, *Recl. Trav. Chim. Pays-Bas* **1964**, *83*, 776–783.
[6] C. J. Müller, T. Doert, U. Schwarz, *Z. Kristallogr. - Cryst. Mater.* **2011**, *226*, 646–650.
[7] C. J. Müller, U. Schwarz, T. Doert, *Z. Anorg. Allg. Chem.* **2012**, *638*, 2477–2484.
[8] K. Stöwe, *J. Alloys Compd.* **2000**, *307*, 101–110.
[9] K. Stöwe, *Z. Anorg. Allg. Chem.* **2000**, *626*, 803–811.
[10] I. Ijjaali, J. A. Ibers, *J. Solid State Chem.* **2006**, *179*, 3456–3460.
[11] L. D. Gulay, J. Stępień-Da mm, M. Daszkiewicz, A. Pietraszko, *J. Alloys Compd.* **2007**, *427*, 166–170.
[12] Y. Wu, T. Doert, P. Böttcher, *Z. Anorg. Allg. Chem.* **2002**, *628*, 2216–2216.
[13] H. Poddig, T. Donath, P. Gebauer, K. Finzel, M. Kohout, Y. Wu, P. Schmidt, T. Doert, *Z. Anorg. Allg. Chem.* **2018**, *644*, 1886–1896.
[14] Y. S. Shin, C. W. Han, B. H. Min, H. J. Lee, C. H. Choi, Y. S. Kim, D. L. Kim, Y. S. Kwon, *Phys. B* **2000**, *291*, 225–227.
[15] B. H. Min, H. Y. Choi, Y. S. Kwon, *Phys. B* **2002**, *312–313*, 203–204.
[16] K. Y. Shin, V. Brouet, N. Ru, Z. X. Shen, I. R. Fisher, *Phys. Rev. B* **2005**, *72*, 085132.
[17] D. R. Garcia, S. Y. Zhou, G.-H. Gweon, M. H. Jung, Y. S. Kwon, A. Lanzara, *J. Electron Spectrosc. Relat. Phenom.* **2007**, *156–158*, 58–63.
[18] M. H. Jung, Y. S. Kwon, T. Kinoshita, S. Kimura, *Phys. B* **1997**, *230–232*, 151–154.
[19] M. Lavagnini, A. Sacchetti, L. Degiorgi, K. Y. Shin, I. R. Fisher, *Phys. Rev. B* **2007**, *75*, 205133.
[20] M. Lavagnini, A. Sacchetti, L. Degiorgi, E. Arcangeletti, L. Baldassarre, P. Postorino, S. Lupi, A. Perucchi, K. Y. Shin, I. R. Fisher, *Phys. Rev. B* **2008**, *77*, 165132.
[21] Y. S. Kwon, B. H. Min, *Phys. B* **2000**, *281–282*, 120–121.
[22] B. H. Min, E. D. Moon, H. J. Im, S. O. Hong, Y. S. Kwon, D. L. Kim, H.-C. Ri, *Phys. B* **2002**, *312–313*, 205–207.
[23] A. F. May, J.-P. Fleurial, G. J. Snyder, *Phys. Rev. B* **2008**, *78*, 125205.
[24] X. Wang, R. Yang, Y. Zhang, P. Zhang, Y. Xue, *Appl. Phys. Lett.* **2011**, *98*, 222110.
[25] D. Cheikh, B. E. Hogan, T. Vo, P. Von Allmen, K. Lee, D. M. Smiadak, A. Zevalkink, B. S. Dunn, J.-P. Fleurial, S. K. Bux, *Joule* **2018**, *2*, 698–709.
[26] S. J. Gomez, D. Cheikh, T. Vo, P. Von Allmen, K. Lee, M. Wood, G. J. Snyder, B. S. Dunn, J.-P. Fleurial, S. K. Bux, *Chem. Mater.* **2019**, *31*, 4460–4468.
[27] R. Niewa, A. Czulucki, M. Schmidt, G. Auffermann, T. Cichorek, M. Meven, B. Pedersen, F. Steglich, R. Kniep, *J. Solid State Chem.* **2010**, *183*, 1309–1313.
[28] T. Cichorek, L. Bochenek, R. Niewa, M. Schmidt, A. Schlechte, R. Kniep, F. Steglich, *J. Phys. Conf., Ser.* **2010**, *200*, 012021.
[29] A. Czulucki, G. Auffermann, M. Bednarski, Ł. Bochenek, M. Böhme, T. Cichorek, R. Niewa, N. Oeschler, M. Schmidt, F. Steglich, et al., *ChemPhysChem* **2010**, *11*, 2639–2644.
[30] T. Cichorek, L. Bochenek, Z. Henkie, M. Schmidt, A. Czulucki, R. Kniep, F. Steglich, *Phys. Status Solidi B* **2010**, *247*, 586–588.
[31] A. Czulucki, Struktur-/Eigenschafts-Beziehungen in ternären Übergangs- und Seltenerdmetall-Pniktid-Chalkogeniden, Phd Thesis, Technische Universität Dresden, **2010**.
[32] P. Böttcher, T. Doert, H. Arnold, R. Tamazyan, *Z. Kristallogr. - Cryst. Mater.* **2000**, *215*, 246–253.
[33] C. Bartsch, T. Doert, *J. Solid State Chem.* **2012**, *185*, 101–106.
[34] C. Bartsch, T. Doert, *Solid State Sci.* **2012**, *14*, 515–521.
[35] L. Pauling, *The Nature of the Chemical Bond*, Cornell University Press, Ithaca, New York, **1960**.
[36] L. C. Allen, *J. Am. Chem. Soc.* **1989**, *111*, 9003–9014.
[37] A. L. Allred, E. G. Rochow, *J. Inorg. Nucl. Chem.* **1958**, *5*, 264–268.
[38] S. Lei, V. Duppel, J. M. Lippmann, J. Nuss, B. V. Lotsch, L. M. Schoop, *Adv. Quantum Technol.* **2019**, *0*, 1900045.
[39] F. Q. Huang, P. Brazis, C. R. Kannewurf, J. A. Ibers, *Inorg. Chem.* **2000**, *39*, 3176-3180.
[40] J. C. Slater, *J. Chem. Phys.* **1964**, *41*, 3199–3204.
[41] F. Pabst, D. Hobbis, N. Alzahrani, H. Wang, I. P. Rusinov, E. V. Chulkov, J. Martin, M. Ruck, G. S. Nolas, *J. Appl. Phys.* **2019**, *ADVTHRM2019*, 105105; DOI: 10.1063/1.5116369.
[42] G. S. Nolas, J. Sharp, J. Goldsmid, *Thermoelectrics: Basic Principles and New Materials*, Springer-Verlag, Berlin, Heidelberg, **2001**.
[43] Y. Dong, H. Wang, G. S. Nolas, *Phys. Status Solidi RRL* **2014**, *8*, 61–64.
[44] K. Wei, G. S. Nolas, *ACS Appl. Mater. Interfaces* **2015**, *7*, 9752–9757.
[45] J. Martin, S. Erickson, G. S. Nolas, P. Alboni, T. M. Tritt, J. Yang, *J. Appl. Phys.* **2006**, *99*, 044903.
[46] J. Martin, G. S. Nolas, *Rev. Sci. Instrum.* **2016**, *87*, 015105.

Received: March 2, 2020